

CONNECTING SURFACE WEATHER OVER NORTH AMERICA TO THE MID-LATITUDE SEASONAL OSCILLATION

by

Zachary H Manthos
A Thesis
Submitted to the
Graduate Faculty
of
George Mason University
in Partial Fulfillment of
The Requirements for the Degree
of
Master of Science
Climate Science

Committee:

_____ Dr. Kathleen Pegion, Thesis Chair
_____ Dr. Paul Dirmeyer, Committee Member
_____ Dr. Cristiana Stan, Committee Member
_____ Dr. James Kinter, Department Chairperson
_____ Dr. Donna M. Fox, Associate Dean, Office
of Student Affairs & Special Programs,
College of Science
_____ Dr. Fernando Miralles-Wilhelm, Dean,
College of Science

Date: _____ Spring Semester 2021
George Mason University
Fairfax, VA

Connecting Surface Weather over North America to the Mid-latitude Seasonal
Oscillation

A Thesis submitted in partial fulfillment of the requirements for the degree of Master of
Science at George Mason University

by

Zachary H Manthos
Bachelor of Science
George Mason University, 2017
Bachelor of Science
Virginia Commonwealth University, 2014

Director: Kathleen V. Pegion, Assoc. Professor
Atmospheric, Oceanic, and Earth Science

Spring Semester 2021
George Mason University
Fairfax, VA

Copyright 2021 Zachary H Manthos
All Rights Reserved

ACKNOWLEDGEMENTS

I would like to thank my family, friends, and supporters who have made this possible. This could not have been completed without the invaluable help and knowledge from my advisors Dr. Kathleen Pegion and Dr. Cristiana Stan. Dr. Paul Dirmeyer, a committee member, was also immensely helpful and provided unique insights that made this happen. Finally, I want to thank the whole GMU AOES department for supporting me through this.

TABLE OF CONTENTS

	Page
List of Tables	vi
List of Figures	vii
List of Equations	ix
List of Abbreviations	x
Abstract	xi
Chapter One	1
Introduction	1
Chapter Two.....	6
Data	6
GPCP	6
ERA5	7
Era-Interim.....	7
Indices.....	7
Chapter Three.....	9
Methods.....	9
Chapter Four	15
Results	15
MLSO	16
Temperature	16
Precipitation	20
Multi-Oscillation Analyses	24
Temperature	25
Precipitation	28
Chapter Five.....	32
Discussion	32
Chapter Six.....	35
Conclusion.....	35
Appendix.....	36
References.....	43

Biography..... 45

LIST OF TABLES

	Page
Table	
Table 1 - Table showing the information about the indices.....	8
Table 2 - Structure of Analyses	11

LIST OF FIGURES

Figure	Page
Figure 1 - Space-time structure of the MLSO (Fig. 3-A, Stan & Krishnamurthy, 2019)...	4
Figure 2 - Time series of the MLSO index with the bins used in the study shaded to the corresponding color. The dividing lines between bins are $y = 0.75, 0, -0.75$. The index is based on the 500-hPa geopotential height daily anomalies. The values of the index are standardized	10
Figure 3 - Temperature Distribution for the location 53N 115 W for the MLSO alone during the winter. The red line a zero line, the dashed line is the average, and the solid black line is the median, a proxy for the ratio.....	17
Figure 4 - The average temperature anomalies for the MLSO, split into the index bins used in figure 2, strong positive (top) to strong negative (bottom), for the boreal winter season, October – March.....	17
Figure 5 - The temperature ratios for the MLSO, split into the index bins used in figure 2, strong positive (top) to strong negative (bottom), for the boreal winter season, October – March	17
Figure 6 - Geopotential height anomalies for the 500 hPa level for the MLSO alone during the winter split into the index bins used in figure 2	18
Figure 7 - The highest (top) and lowest (bottom) temperature ratio for a particular point plotted as the bin the ratio occurred in during the boreal winter season, October – March. Stippling denotes significance passing an FDR test at $\alpha=0.05$	20
Figure 8 - The highest (top) and lowest (bottom) average temperature anomaly for a particular point plotted as the bin the anomaly occurred in during the boreal winter season, October – March. Stippling denotes significance passing an FDR test at $\alpha=0.05$ 20	20
Figure 9 - The precipitation ratios for the MLSO alone, split into the index bins used in figure 1, strong positive (top) to strong negative (bottom), for the boreal summer season, April – September	21
Figure 10 - The average precipitation anomalies for the MLSO alone, split into the index bins used in figure 1, strong positive (top) to strong negative (bottom), for the boreal summer season, April – September	21
Figure 11 - The highest (top) and lowest (bottom) average precipitation anomaly for a particular point plotted as the bin the anomaly occurred in during the boreal summer, April – September. Stippling denotes significance passing an FDR test at $\alpha=0.1$	23
Figure 12 - The highest (top) and lowest (bottom) average precipitation anomaly for a particular point plotted as the bin the anomaly occurred in during the boreal summer, April – September. Stippling denotes significance passing an FDR test at $\alpha=0.1$	23
Figure 13 - The temperature ratios for the ENSO alone, split into the index bins used in figure 2, strong positive (top) to strong negative (bottom), for the boreal winter season, October – March	25

Figure 14 - The average temperature anomalies for the ENSO alone, split into the index bins used in figure 2, strong positive (top) to strong negative (bottom), for the boreal winter season, October – March	25
Figure 15 - The MLSO and ENSO out of phase combination, split into the bins used in figure 1, for the average temperature anomalies during the boreal winter, October – March	26
Figure 16 - The MLSO and ENSO out of phase combination, split into the bins used in figure 1, for the temperature ratios during the boreal winter, October – March.....	26
Figure 17 - The precipitation ratios for the ENSO alone, split into the index bins used in figure 1, strong positive (top) to strong negative (bottom), for the boreal summer season, April – September	29
Figure 18 - The average precipitation anomalies for the ENSO alone, split into the index bins used in figure 1, strong positive (top) to strong negative (bottom), for the boreal summer season, April – September	29
Figure 19 - The MLSO and ENSO in phase combination, split into the bins used in figure 1, for the precipitation ratios during the boreal summer, April – September	30
Figure 20 - The MLSO and ENSO in phase combination, split into the bins used in figure 1, for the average precipitation anomalies during the boreal summer, April – September	30

LIST OF EQUATIONS

Equation	Page
Equation 1 - Example of How the Bins are split for the statistical tests.....	12
Equation 2 - Memory for Temperature and Precipitation.....	13

LIST OF ABBREVIATIONS

Binomial Proportion Test	BPT
Climate Prediction Center	CPC
Degrees of Freedom	DOF
ECMWF Reanalysis 5th Generation	ERA5
European Center for Medium-Range Weather Forecasts	ECMWF
El Niño Southern Oscillation	ENSO
False Discovery Rate	FDR
Global Precipitation Climatology Project	GPCP
Mid-Latitude Seasonal Oscillation	MLSO
Mid-Latitude Intra-Seasonal Oscillation	MLISO
Multi-channel Single Spectrum Analysis	MSSA
National Oceanic and Atmospheric Association	NOAA
North Atlantic Oscillation	NAO
NOAA Optimum Interpolation Sea Surface Temperature	OISST
Pacific North American teleconnection pattern	PNA
Ratio Anomaly Inversion	RAI
Rotated Principal Component Analysis	RPCA
Wilcoxon Rank-Sum test	WRS

ABSTRACT

CONNECTING SURFACE WEATHER OVER NORTH AMERICA TO THE MID-LATITUDE SEASONAL OSCILLATION

Zachary H Manthos, M.S.

George Mason University, 2021

Thesis Director: Dr. Kathleen V. Pegion

The 120-day Mid-latitude Seasonal Oscillation (MLSO) and its possible connections to surface weather over North America are investigated. Atmospheric modes, such as the North Atlantic Oscillation (NAO), Pacific North American (PNA) teleconnection pattern, and the atmosphere-ocean coupled mode El Niño Southern Oscillation (ENSO), are known to have significant impacts on surface weather, e.g., temperature and precipitation. Understanding how the recently discovered MLSO affects the surface weather over North America will be useful for improving the extended-range forecast. The analysis of frequency ratios such as warm over cold days and wet over dry days and composite analysis reveal the influence of MLSO on surface weather. The impact of MLSO is also investigated in conjunction with other climate modes such as NAO, PNA and ENSO. All investigations are split into boreal summer and winter and the analyses of the MLSO combined with other modes are conducted for two modes of phasing: in phase and out of phase. These analyses reveal that the MLSO is an important factor in understanding the temperature variability over North America. It is also found

that the MLSO plays a role in exciting variability when interacting with other modes exerting influence over the same region. Expected patterns of temperature and precipitation associated with well-known climate modes show deviation when they are further decomposed to account for the MLSO influence. The MLSO is a vital component to the climate system of North America and its affects elsewhere on the globe need to be investigated.

CHAPTER ONE

Introduction

Mid-latitude surface weather (e.g., precipitation and surface air temperature) is influenced by small-scale, local effects (e.g., land-atmosphere interactions), and large-scale patterns of pressure and circulation anomalies. The subseasonal-to-seasonal variability of surface weather can be partially attributed to recurring long-lived pressure patterns, also known as atmospheric oscillations, and tropically forced large-scale pressure anomalies, known as teleconnection patterns. Atmospheric oscillations have been in the view of the scientific community since the late 19th century but had not been realized until the 1932 paper by Walker and Bliss. Walker and Bliss (1932) used the noticeable effects of atmospheric oscillations on surface pressure, temperature, and precipitation to define them. They discussed the North Atlantic Oscillation (NAO), North Pacific Oscillation an integral part of the Pacific North American pattern (PNA), and the Southern Oscillation now known as the El Niño Southern Oscillation (ENSO). Subsequent research has gone on to solidify these atmospheric oscillations and teleconnection patterns as important pieces of our climatic system (Wallace & Gutzler, 1981; Leathers et al., 1991; Diaz et al., 2001; etc.).

Many research studies have shown strong relationships between atmospheric modes of variability, e.g., atmospheric oscillations and teleconnection patterns, and precipitation and temperature anomalies. The NAO has a dipole structure over the North Atlantic with surface pressure centers over Greenland and the Azores (Walker & Bliss,

1932). The strength of the pressure centers defines the oscillation and has a profound impact on the wind field over the North Atlantic (Walker & Bliss, 1932; Wallace & Gutzler, 1981; Hurrell & Dickinson, 2004). The changes in both pressure and wind cause precipitation and temperature anomalies across the northeast coast of North America and Europe (Hurrell & Dickinson, 2004; Durkee et al., 2008; Kenyon & Hegerl, 2008; Bonsal & Shabbar, 2008).

The PNA teleconnection pattern arises from pressure variations over the North Pacific, which have a strong connection to tropical variability. The PNA is a main influencer of the climate system of North America and has been shown to have a larger impact than the NAO across most of the continent (Archambault et al., 2008; Ning & Bradley, 2014). This is due to North America being downstream from the origins of the PNA and upstream from the NAO. The changes in pressure related to the PNA affect the jet stream location over North America, and that in turn can lead to conditions that create notable precipitation and temperature anomalies.

ENSO is a coupled ocean-atmosphere phenomena in the tropical Pacific that influences North America. Unlike the NAO and PNA, ENSO is a longitudinal oscillation of pressure and ocean surface temperature in the equatorial Pacific. The location of ENSO gives it the unusual power of being able to affect the entire globe and it has a well-known link to precipitation and temperature anomalies over North America (Diaz et al., 2001; Kenyon & Hegerl, 2008; Bonsal & Shabbar, 2008; X. Zhang et al., 2010; Ning & Bradley, 2014).

The NAO, PNA, ENSO, and many other atmospheric modes are used by forecasters to inform their forecasts but due to their seasonal timescales they are limited in what information they can provide for weather forecasts. The persistent nature of these phenomena leads to changes in climate, monthly to yearly time scales, and not the day-to-day weather. Typical deterministic weather forecasts have a predictability limit of about 10 days (Pegion & Sardeshmukh, 2011), and with the long time scales, a few months and longer, of most atmospheric modes there is a gap between weather and probabilistic climate forecasts. A recent study by Osman et al. (2021) shows that the NAO is significantly correlated to temperature at seasonal and sub-seasonal timescales over eastern North America and Europe. The correlations were stronger in the winter, but summer still had large areas of significant correlations. In the study, they also analyzed the NAO pressure field to multiple NAO indices at a wide range of time scales, seasonal to sub-monthly. At the sub-monthly time scale, 10-day running mean, they were able to find significant correlations between the NAO and various indices but they were much weaker than those of the longer time scales, monthly and longer. This was thought to be due to NAO indices, at the 10-day time scale, capturing the movement of the weather systems moving across the Atlantic (Osman et al., 2021). Identifying new modes of atmospheric variability at these time scales and identifying and discerning the effects of the atmospheric modes at seasonal to sub-seasonal time scales could prove useful for improving prediction capabilities.

In an article by Stan and Krishnamurthy (2019), three new seasonal to sub-seasonal oscillations have been identified. These oscillations were found in the Northern

Hemisphere mid-latitudes and together can explain up to 30% of the natural variability for the sub-seasonal to seasonal time scales (Stan & Krishnamurthy, 2019). The one seasonal and two intra-seasonal oscillations have average periods of 120 (MLSO), 45 (MLISO-1), and 28 (MLISO-2) days respectively. MLSO was shown to correlate strongly (>0.8) with the NAO for 6 out of 8 phases in its cycle over the north Atlantic. The MLISO-1 is strongly correlated to the PNA for 4 out of 8 phases over the north Pacific and North America. The strong similarities between these atmospheric modes raises the question of whether they have similar effects on the weather and climate.

The MLSO is the focus of this study because it resembles the well-known NAO but also because it has structure outside of the North Atlantic dipole (Fig. 1) that could give it a larger area of influence. Along with the North Atlantic dipole, there is a strong pressure center over northeastern Europe and Siberia that has a sign equal to the pressure center over the Aleutian Islands. Although not as strong as the dipole over the North

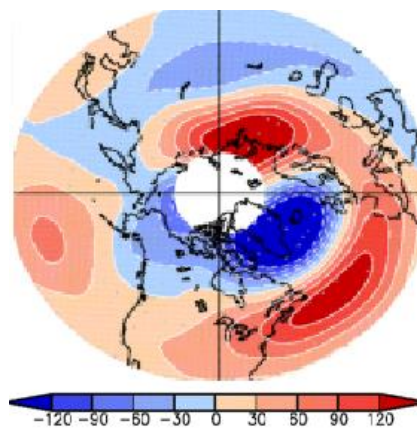


Figure 1 - Space-time structure of the MLSO (Fig. 3-A, Stan & Krishnamurthy, 2019)

Atlantic there is a dipole structure over the North Pacific that matches the signs of the structure over the North Atlantic (Stan & Krishnamurthy, 2019). Having features both upstream and downstream of North America means that there is a strong potential for the MLSO to have an influence over the climate of North America. The MLSO has the potential to impact surface weather over North America, so the possible connections between the different phases of the MLSO and temperature and precipitation will be the focus of this study.

The objective of this study is to determine if North American temperature and precipitation is related to the MLSO. Knowing that the NAO, PNA, and ENSO all have influence over the climate of North America, the MLSO may also have an influence over the continent. Temperature and precipitation vary for many reasons, and the methods used in this study aim to reveal if the MLSO has a noticeable influence over them. The results of this study will show how the probability and magnitude of temperature and precipitation anomalies vary in accordance with different phases of the MLSO.

CHAPTER TWO

Data

This study uses 2m surface air temperature, precipitation, 500 hPa pressure heights, and sea surface temperature for the analysis. The domain of focus is North America and the area analyzed is the region spanning 25°-55°N, 130°-50°W. The time span of the analysis starts in 1997 and goes through 2018, 22 years. The datasets that are used are the Global Precipitation Climate Project (GPCP) V1.3 One-Degree Daily (Huffman et al., 2001), ECMWF Reanalysis 5th Generation (ERA5) (Hersbach et al., 2020), ERA-Interim (Dee et al., 2011), and indices for the MLSO Stan and Krishnamurthy (2019), NAO and PNA from https://www.cpc.ncep.noaa.gov/products/precip/CWlink/daily_ao_index/teleconnections.shtml, and ENSO calculated in this study.

GPCP

The GPCP V1.3 dataset is a daily observationally based global precipitation dataset that has a 1° x 1° resolution. The data is constructed using measurements from infrared radiometers on geosynchronous satellites, for the region 40°S to 40°N, and from sounding data from low-earth polar-orbit satellites, for the rest of the globe. GPCP V1.3 has been tested for validation multiple times across different climates and topographies and has been shown to perform well (Huffman et al., 2001).

ERA5

The ERA5 dataset is a fifth-generation atmospheric reanalysis (Hersbach et al., 2020) that supplies the 2m surface temperature used for this study. This reanalysis is an improvement on previous generation for both temporal and spatial resolutions. The full reanalysis has a spatial resolution of 31 km, 137 atmospheric levels, and has hourly output. The dataset used in this study is a modified version with land only grid points and a daily temporal resolution, where the daily values are the average of the hourly data for a given day.

Era-Interim

The ERA-Interim dataset is a fourth-generation reanalysis (Dee et al., 2011) and supplies the 500 hPa pressure level heights. This reanalysis has a horizontal resolution of 79 km and 60 atmospheric levels. The upper air parameters have 6 hourly output that was averaged to create daily data.

Indices

The daily MLSO index is computed following Stan and Krishnamurthy (2019). This involves using the ERA-Interim 500hPa height anomalies in the Multi-channel Singular Spectrum Analysis (MSSA) method for the region spanning 0° – 360° and 30° N to 75° N. The NAO and PNA daily indices have been obtained from the Climate Prediction Center of NOAA (NOAA-CPC). These indices have been created using 500hPa height anomalies in a Rotated Principal Component Analysis (RPCA). The ENSO, Niño 3.4, index uses the NOAA Optimum Interpolation (OI) Sea Surface Temperature (SST) V2 (Reynolds et al., 2002) dataset, a weekly SST product. OISST

uses *in situ* and satellite data to compute SSTs at a 1° x 1° resolution. This ENSO index is computed using the area averaged anomalies of the SSTs for the Niño3.4 region, 5°N to 5°S and from 170°W to 120°W, and is standardized (Bamston et al., 1997). This gives a weekly index that is then projected onto a daily times series centered on the date of the weekly data with the 3 days prior and 3 days after having a value equal to the weekly index value. All indices are standardized.

Table 1 - Table showing the information about the indices,
https://www.cpc.ncep.noaa.gov/products/precip/CWlink/daily_ao_index/history/method.shtml

Index	Variable	Region	Method
MLSO	500hPa height anomalies	30°N – 75°N	MSSA
ENSO	Sea Surface Temperature	Nino 3.4 5°N – 5°S 170°W – 120°W	Standardized Average SST Anomaly
NAO	500hPa height anomalies	20°N – 90°N	RPCA
PNA	500hPa height anomalies	20°N – 90°N	RPCA

CHAPTER THREE

Methods

For this study, frequency ratios, averages, and multiple statistical tests are used to analyze possible connections between surface weather and the MLSO. Daily anomalies, for temperature and precipitation are created by removing a climatology. The climatology is calculated as the average value for a given day over all 22 years of data. Since the amplitude of the MLSO index tends to be larger during the winter than summer (Stan & Krishnamurthy, 2019), all analyses are also split into boreal summer and boreal winter seasons. The boreal winter is defined as October through March and the boreal summer as April through September. The standardized MLSO index has been categorized into four bins corresponding to four states of the MLSO: strong positive, weak positive, weak negative, and strong negative (Fig. 2). Strong bins have the lower magnitude limit of 0.75, index value, and have no upper limit and the weak bins span 0.75 to 0, index value, for their respective sign. The threshold of 0.75 is used to ensure reasonably large sample sizes for the strong bins. Splitting the typical neutral bin, 1 to -1 index value, into the two weak bins may reveal more information than would typically be seen in a single bin.

The investigation into the possible connection between MLSO and precipitation and temperature, two procedures are used with multiple configurations. An analysis of frequency ratios is performed to determine the impact of the MLSO on the preference for warm vs. cold, anomaly, or wet vs. dry, total value, days. The frequency ratio is

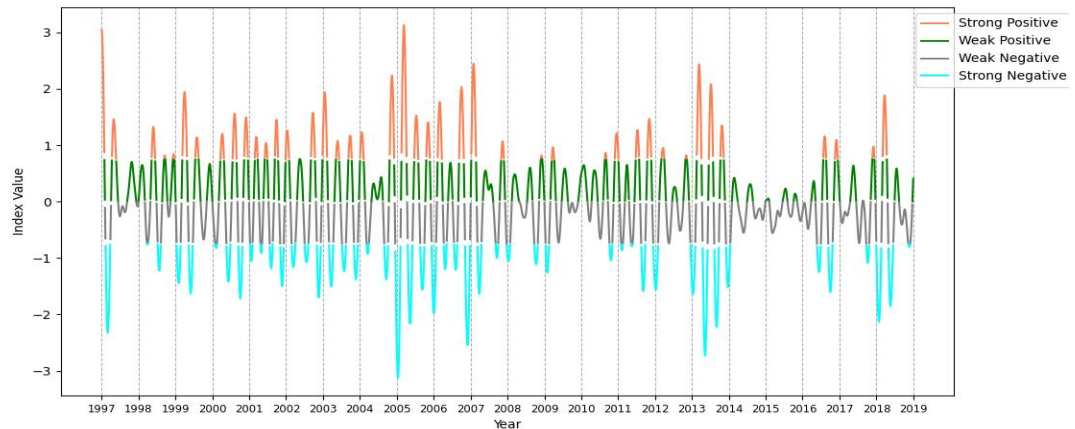


Figure 2 - Time series of the MLSO index with the bins used in the study shaded to the corresponding color. The dividing lines between bins are $y = 0.75, 0, -0.75$. The index is based on the 500-hPa geopotential height daily anomalies. The values of the index are standardized

calculated as the number of wet days over the number of dry days or warm days over cold days. The threshold for classifying a particular day as a warm or cold day is a temperature anomaly of 0.0°C . The threshold for classification of a particular day as a wet or dry day is 0.01 mm/day based on the total precipitation. This threshold is used for precipitation because it will exclude days that have small precipitation events and emphasize larger precipitation events, which are most important for quantifying the potential large-scale impact of the MLSO on precipitation. The 0.01 mm/day is selected because it is much less than the 0.3 mm/hour , the maximum of a light drizzle as defined by of American Meteorological Society (Drizzle - Glossary of Meteorology. (2012, January 26). Retrieved October 18, 2020, from <https://glossary.ametsoc.org/wiki/Drizzle>) and values between 0.01 mm/day and 0 mm/day only make up about 1% of the data. Only the precipitation ratios will use the total value with all other analyses using anomalies.

Averages of the anomalies of precipitation and temperature for different MLSO bins are used to investigate the impact of the MLSO on the magnitude of precipitation or temperature. The precipitation anomalies are calculated with no alteration of the original data, i.e., no threshold is imparted on small values.

These two analyses, frequency ratios and averages, are applied to precipitation and temperature for the four bins of the MLSO. They are also applied to combinations of MLSO bins with NAO, PNA, and ENSO to investigate the impact of the MLSO in combination with these other teleconnection and oscillation patterns. For these combinations, the MLSO and only one other index is combined at a time. The combination approach for the indices uses the days associated with each bin based on whether the MLSO and other index are in phase or out of phase. In phase is defined as when the signs of each index are the same and out of phase is when they are opposite. Once selected, the ratio and average analyses are applied.

Table 2 - Structure of Analyses

Configurations	Procedure 1: Frequency Ratios	Procedure 2: Averages
	MLSO Alone	MLSO Alone
	MLSO + ENSO in and out of phase	MLSO + ENSO in and out of phase
	MLSO + NAO in and out of phase	MLSO + NAO in and out of phase
	MLSO + PNA in and out of phase	MLSO + PNA in and out of phase

In order to determine the significance of results, two statistical tests are employed. These tests are applied to the analysis of the MLSO, not in combination with the other atmospheric modes. Both tests identify the bin that exhibited the highest (lowest) ratio or average anomaly versus all the other bins combined. For example, in equation 1 below, A_1 represents the highest average of temperature anomalies, e.g., present in the strong positive bin, and A_{234} represents the value A_1 is tested against. A_{234} is an average of temperature using all the data selected for the other bins; weak positive, weak negative, and strong negative. This tests the selected bin, A_1 , against all the other data, A_{234} , to determine if A_1 is statistically different from A_{234} .

Equation 1 - Example of How the Bins are split for the statistical tests

$$A_1 \text{ vs } A_{234} = \frac{D_2 + D_3 + D_4}{N_2 + N_3 + N_4}$$

Where:

A_1 = Highest Average found in bin 1

A_{234} = Average for bins 2-4

D_{2-4} = Anomaly values for other bins

N_{2-4} = Total number of data points in bins 2-4

First, a binomial proportion test (BPT; D'Agostino et al., 1988) is used to determine p-values for the ratios of wet to dry or warm to cold. The BPT is a simplified version of a Student's t-test where there are only 2 possible outcomes. With the BPT applied to a time series, there is need to reduce the degrees of freedom (DOF) because of autocorrelation in time that could be present in the temperature anomalies and precipitation values. In order to determine the reduction factor for the DOFs, an e-folding

timescale or day-to-day persistence, i.e., memory, in the daily time series of precipitation and temperature fields is calculated (Eq. 2). The first step in determining the memory is to obtain the 1-day lagged auto-correlation for every point in the domain, for one years' worth of data. Then the natural log of the auto-correlation values for every point is found

Equation 2 - Memory for Temperature and Precipitation

$$Mem = \left[\sum_{i=1}^{22} \frac{-1}{Avg_D(\ln acor(x_i))} \right] / 22$$

Where:

Mem = Memory in days

Avg_D = Domain Average

acor = 1-day lagged Auto-Correlation

x_i = Temperature anomalies or Precipitation values for 1 year

and averaged, creating a domain average. Next, negative one is divided by the domain average of the natural log of the auto-correlation values, which gives the domain average memory for a single year. The memory value used in this study is the average of the memories calculated for each year in the study. Temperature has an average memory of 3.4 days, thus reducing its effective sample size by more than two thirds, the inverse of 3.4 times the DOF. Precipitation has a memory of 0.59 days and is determined to be random enough to not warrant a manipulation of the DOF, as it would increase the number of DOF.

Second, the Wilcoxon Rank-Sum test (WRS; Virtanen et al., 2020) is used to show differences in the precipitation anomalies and temperature anomalies between

different bins. Use of this non-parametric test helps to reduce overstating the results and eliminates the need for assumptions about the distribution of the dataset. Both statistical tests provide p-values and in order to determine if any particular p-value is significant at a specified level, the False Discovery Rate (FDR) field significance test is used (Wilks, 2011). The confidence levels for the FDR are 95%, $\alpha = 0.5$ for temperature, and 90%, $\alpha = 0.1$ for precipitation. There are different levels of significance for temperature and precipitation because precipitation is inherently more random, as seen in the difference in the memories. The goal of this study is to determine how and where the MLSO projects its impacts and not to definitively attribute variability in a small area to the MLSO.

CHAPTER FOUR

Results

The investigation into the connections between the MLSO and the environmental variables temperature and precipitation revealed many features; in this chapter a select few analyses are discussed. The selection is intended to limit the number of scenarios discussed but maximize the number of features that can be discussed. The relationships between the MLSO and temperature and precipitation are described first with the boreal winter temperature scenario followed by the boreal summer precipitation scenario. Then the combination of the MLSO and ENSO, and its relationships, are described to illustrate what happens when multiple atmospheric modes are considered at the same time. Results for the MLSO analyses are described in two ways, first, how the frequency ratios relate to the anomalies for the same bin, i.e., strong positive ratios vs. strong positive anomalies. Then the different MLSO bins are compared, i.e., strong positive ratios vs. weak positive ratios, etc., to see how the states of the MLSO vary. For the analyses combining the MLSO with another atmospheric mode, the results are presented similar to the MLSO alone but also include a comparison of the patterns from the indices in question to the patterns from their combination, e.g., MLSO & ENSO vs. MLSO+ENSO. All results are split into two 6-month seasons and the results combining MLSO with another mode of variability are also shown separately for in-phase and out-of-phase.

MLSO

Temperature

The first analysis investigates the winter temperature ratios (Fig. 3) and anomalies (Fig. 4) associated with the four MLSO states. This scenario is chosen because the features it reveals are well defined and the variation between the MLSO states is pronounced. One of the most obvious features that is seen when comparing the panels in the figures is the transition from cold temperature for strong positive MLSO, over most of the domain, to warm for strong negative MLSO, most notably over the eastern US. This shows the MLSOs' oscillatory nature and it can also be seen in the well-defined region in northeast Canada with an opposite sign oscillation. The oscillatory nature is more defined in the averages than the ratios. In western Canada and in the northwestern US there are warm ratios that do not align with the cold anomalies, in the positive states of the MLSO. In these areas there is a skewing of the temperature distribution which can be seen as a negative skew in figure 5. Figure 5 is a histogram of the temperature data at 53°N, 113°W for the weak positive MLSO state and it shows the skew of the temperatures. The highest frequency temperatures are in the low positive values but there are more frequent larger magnitude negative values. The red line is the zero mark, the black line is the median, a proxy for the ratios, and the dashed line is the average. With these three lines it is clear to see the transition from a positive ratio, median, to a negative average, which is what is seen in weak positive state of figures 3 and 4. Another incongruity found are the areas in the southwest US for weak positive and strong negative states of the MLSO (Fig. 4) that show temperature anomalies with the opposite sign

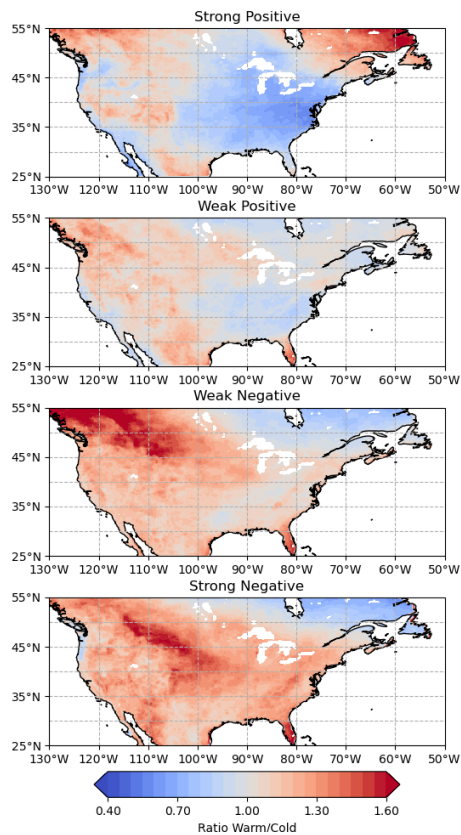


Figure 5 - The temperature ratios for the MLSO, split into the index bins used in figure 2, strong positive (top) to strong negative (bottom), for the boreal winter season, October – March

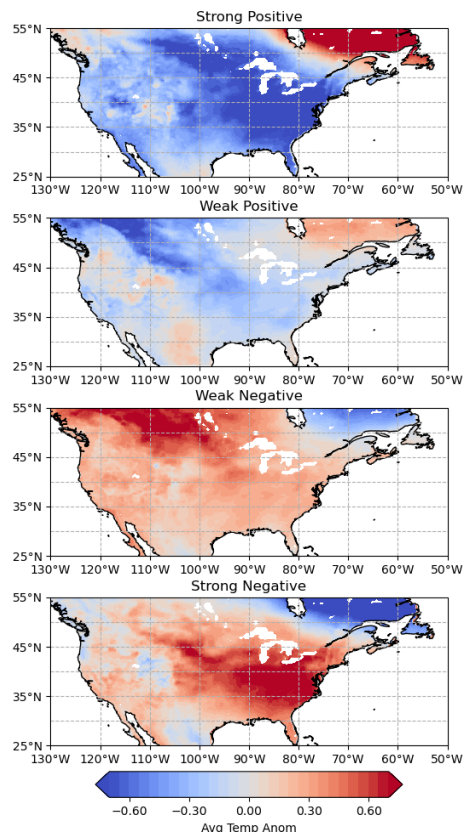


Figure 4 - The average temperature anomalies for the MLSO, split into the index bins used in figure 2, strong positive (top) to strong negative (bottom), for the boreal winter season, October – March

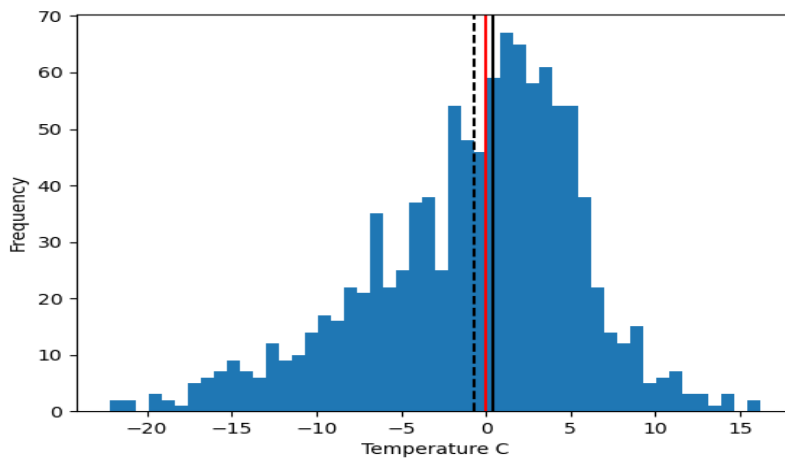


Figure 3 - Temperature Distribution for the location 53N 115 W for the MLSO alone during the winter. The red line a zero line, the dashed line is the average, and the solid black line is the median, a proxy for the ratio

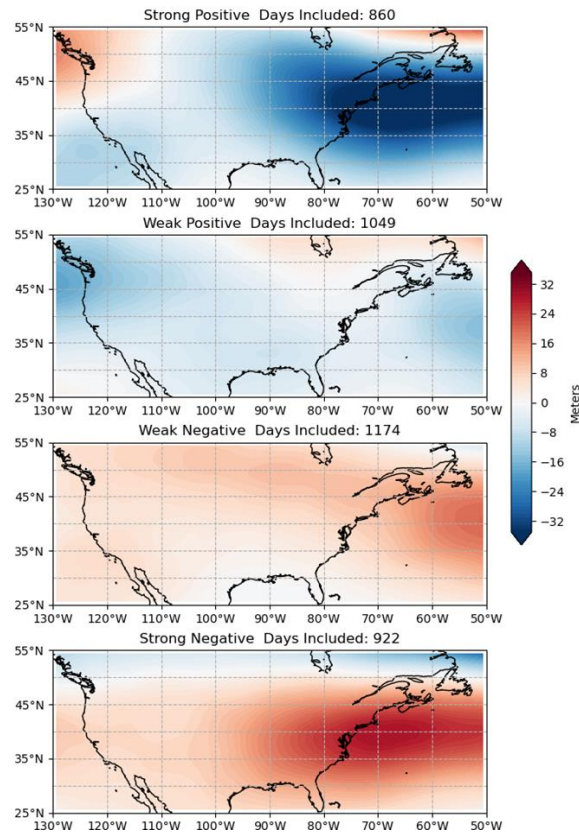


Figure 6 - Geopotential height anomalies for the 500 hPa level for the MLSO alone during the winter split into the index bins used in figure 2

of what is seen for most of the domain. There seems to be an asymmetrical response to the oscillation for these areas in these bins. In order to understand this response, the average 500 hPa geopotential height anomaly is analyzed for each MLSO bin (Fig. 6). The geopotential height anomaly also confirms the MLSO oscillation, but it notably does not show any deviation from the majority of the domain in the southwest US for any bin. This leads to the thought that the anomalies in the southwest US in the weak positive and strong negative bins is most likely due to local features, with the topography being a likely candidate. Figure 6 helps confirm the effect of MLSO oscillation by showing the

sign of geopotential height anomaly across most of North America switch sign when the MLSO index switches sign.

For each location on the domain there are 4 frequency ratios and 4 averages that correspond to the different states of the MLSO. These values are used in order to determine how to split the data for use in the BPT, frequency ratios, and WRS, averages, statistical tests. The significance derived from the BPT, WRS, and FDR tests shows the difference of a single MLSO state from the combination of the rest of the MLSO states. The significance is derived for the MLSO state with the highest, or lowest, ratio or average. Figures 7 and 8 show the MLSO states that have the highest (top) and lowest (bottom) ratio (Fig. 7) and anomaly (Fig. 8). Statistically significant areas are denoted by the stippling. For example, in Figure 7 the highest frequency ratio (top) shows significance in Central Canada, indicating that the strong negative MLSO state (cyan color) is statistically different from all the combined data of the other MLSO states for the summer. This is the methodology for understanding these “application plots”, which show which states of the MLSO have the strongest influence over specific regions of North America.

The application plots (Figs. 7, 8) represent the information seen in figures 4 and 5 in a different way but show similar features. First, the top plots for figures 7 and 8 have most of the domain covered in cyan and grey. These areas are associated with strong negative and weak negative states of the MLSO, respectively. The bottom plots have most of the domain covered in orange and green, showing the strong positive and weak positive states of the MLSO have the largest impact for these locations. These

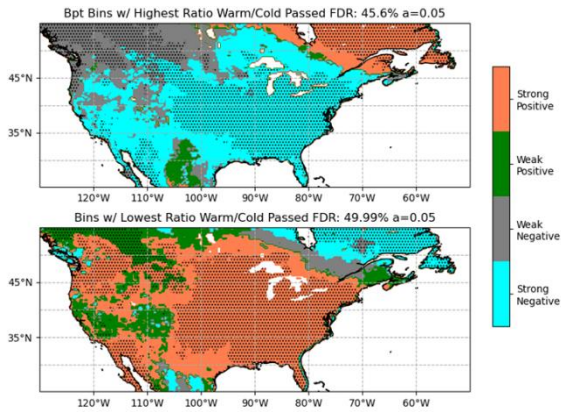


Figure 7 - The highest (top) and lowest (bottom) temperature ratio for a particular point plotted as the bin the ratio occurred in during the boreal winter season, October – March. Stippling denotes significance passing an FDR test at $\alpha=0.05$

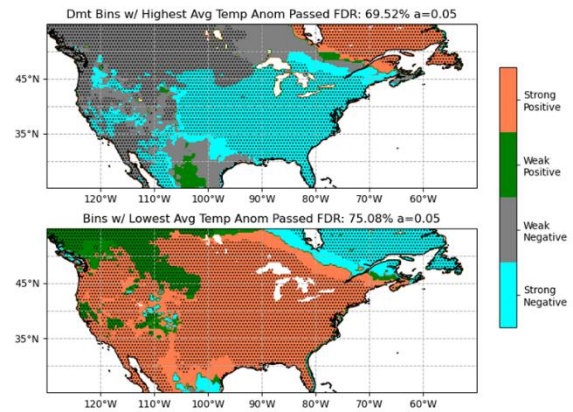


Figure 8 - The highest (top) and lowest (bottom) average temperature anomaly for a particular point plotted as the bin the anomaly occurred in during the boreal winter season, October – March. Stippling denotes significance passing an FDR test at $\alpha=0.05$

differences show a fluctuation between the positive and negative states that corroborates the findings that figures 4 and 5 show the MLSO's oscillatory nature. Second, the large areas that each MLSO state covers hints at a change in the large-scale atmospheric circulation. This is seen in figure 6, where the 500 hPa geopotential height anomalies have a fluctuation in sign between the positive and negative states of the MLSO for large areas over North America. Third, the stippling shows the significance for the different statistical tests, BPT for ratios and WRS for the averages, after being processed by the FDR at significance level of $\alpha = 0.05$. The large areas of stippling signifies that the MLSO has a strong relationship with temperature over North America.

Precipitation

The second part of this investigation is an analysis of the connections between the MLSO and precipitation. An important note and obviously seen in plots of the wet to dry

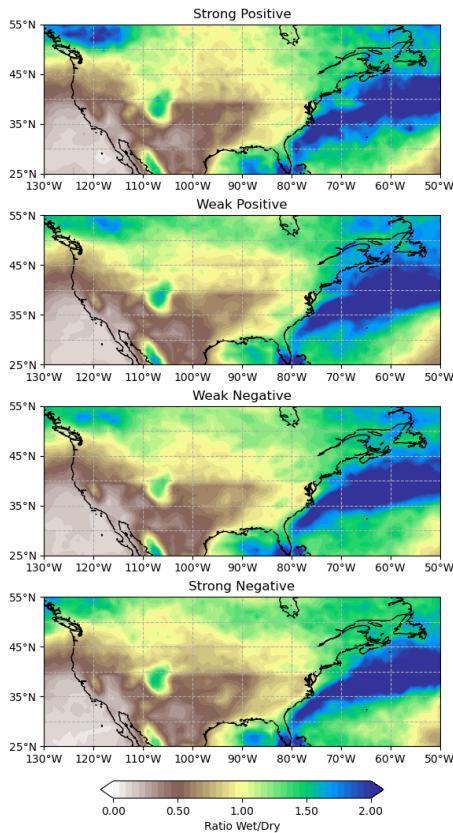


Figure 9 - The precipitation ratios for the MLSO alone, split into the index bins used in figure 1, strong positive (top) to strong negative (bottom), for the boreal summer season, April – September

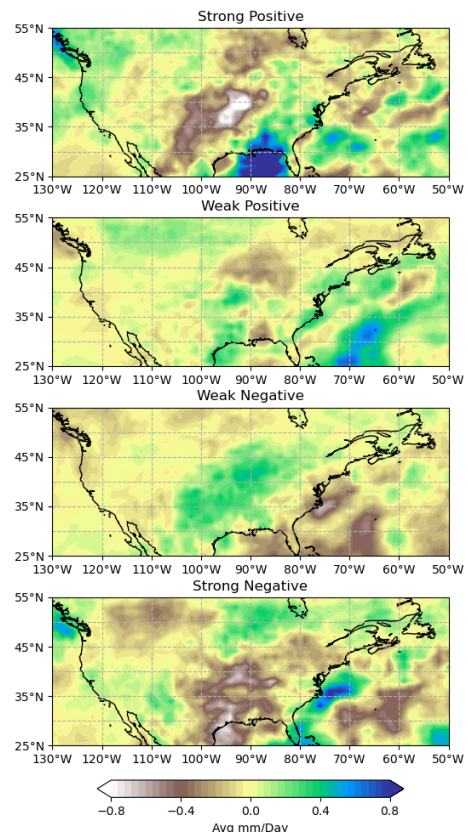


Figure 10 - The average precipitation anomalies for the MLSO alone, split into the index bins used in figure 1, strong positive (top) to strong negative (bottom), for the boreal summer season, April – September

day ratios is the flat “divide” across the US (Fig. 9). This feature is an artifact from the data which had a calculation methodology change at the 40th parallel. While this is very apparent in the ratios, it is not seen in the averages and the data was not altered in response to the revealed artifact.

For the precipitation analysis the summer scenario is described, both summer and winter show evidence of dominance and emergence, but with different spatial patterns.

The comparison between the MLSO bins for the frequency ratios (Fig. 9) shows little variation which means that the MLSO does not have an influence on the frequency of precipitation over most North America. As for the precipitation averages (Fig. 10) there is much more variability between the bins. While there is the possibility of important features with the increased variability, the variability between the MLSO states is relatively chaotic and there is nothing that can be clearly seen as following the MLSO's oscillatory nature. That being said, some areas show a magnitude-based oscillation, i.e., following the absolute value of the MLSO index. The areas that show this type of oscillation are the Pacific off of western Canada and some parts of the central US (Fig.10). In the Pacific and central US the strong MLSO states show the same sign for the average and the weak states show the opposite sign average. The picture that unfolds reveals a few areas that might show a relationship between the MLSO and precipitation, but most areas show patterns that are not easily connected between the states of the MLSO.

Statistical significance was much less present in the precipitation analyses, even with a reduced significance level of $\alpha = 0.1$. Figures 11 and 12 are the same as 7 and 8, but for precipitation, and they show no significance for the ratios and only small significant regions for the averages. This lack of significance shows that MLSO has little definitive influence over North America precipitation. The MLSO is shown to have a statistical connection to precipitation magnitude in a few small areas, mostly over the Atlantic, but for the majority of North America the MLSO can only be thought of as an influencing factor of precipitation based on this analysis. With that being said there is still

information that can be pulled from figures 11 and 12. When looking at figures 9 and 10 there is no noticeable oscillatory patterns but when looking at figures 11 and 12 there is a noticeable flip of signs for the similar patterns seen in figures 11 and 12. The Central US is mostly grey and cyan, positive states, in the top panel of figure 12 but in the bottom panel it is mostly orange and green, negative states, in the same area. This hints at an oscillation between the signs of the MLSO states but the reversal of sign between the top and bottom plots does not appear everywhere. A similar feature is seen in the frequency ratio plots (Fig. 11), however these plots reveal more inconsistencies.

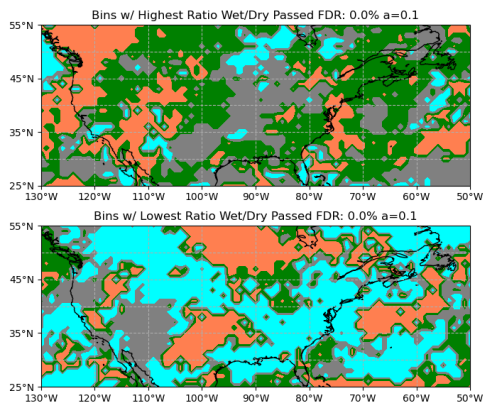


Figure 11 - The highest (top) and lowest (bottom) average precipitation anomaly for a particular point plotted as the bin the anomaly occurred in during the boreal summer, April – September. Stippling denotes significance passing an FDR test at $\alpha=0.1$

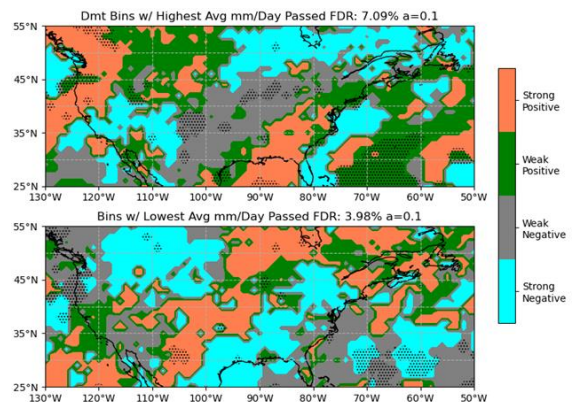


Figure 12 - The highest (top) and lowest (bottom) average precipitation anomaly for a particular point plotted as the bin the anomaly occurred in during the boreal summer, April – September. Stippling denotes significance passing an FDR test at $\alpha=0.1$

Multi-Oscillation Analyses

As mentioned in the Introduction, the variability of surface air temperature and precipitation can be influenced by tropical forcing associated with ENSO and other mid-latitude large-scale recurring patterns such as NAO and PNA. Their individual effects may combine with the MLSO effects and change the precipitation and temperature variability. These analyses will focus on the influence of individual patterns, vs. the combined patterns. The objective is to determine the dominant influence in specific areas, areas where the patterns interfere constructively or destructively, and the emergence of new patterns. The MLSO and ENSO effects on the atmospheric circulation over North America are different from each other and also different from the effects seen when analyzing the combination of the two. The variation of combined effects is evaluated with the same methods as used above and the combinations help to show the interplay between the two atmospheric modes. To show the interplay the scenario that is described for temperature is the out of phase (opposite signed) MLSO + ENSO combination for the boreal winter and for precipitation is the in phase (same signed) MLSO + ENSO combination during the boreal summer. The out of phase winter combination of MLSO and ENSO is chosen because it shows all the features stated above such as dominance, amplification, negation, and emergence and also shows areas of skewed temperature distributions. For the precipitation analysis, the in-phase summer combination of MLSO and ENSO is chosen because it has the most notable changes in the ratios and also large variations in the averages.

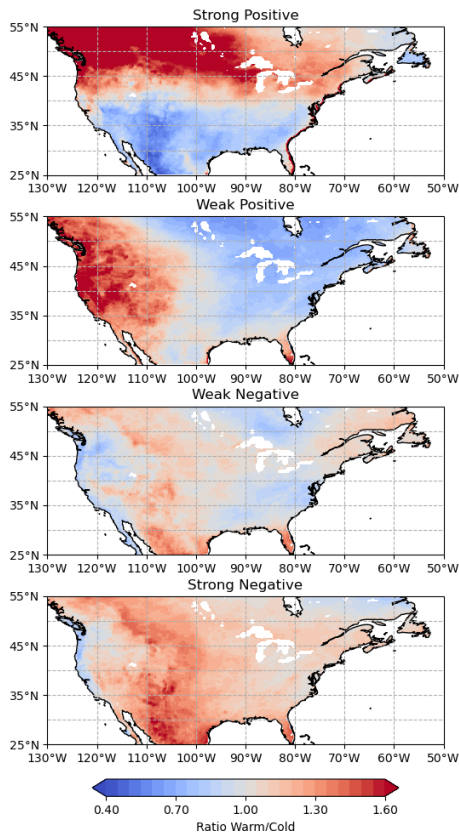


Figure 13 - The temperature ratios for the ENSO alone, split into the index bins used in figure 2, strong positive (top) to strong negative (bottom), for the boreal winter season, October – March

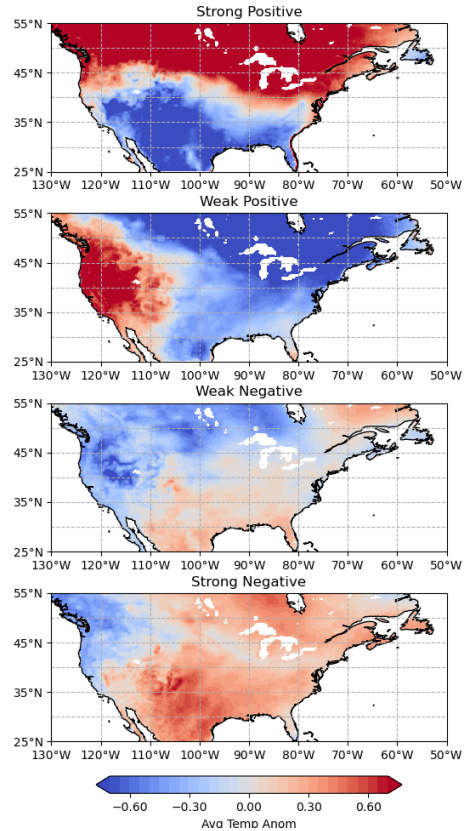


Figure 14 - The average temperature anomalies for the ENSO alone, split into the index bins used in figure 2, strong positive (top) to strong negative (bottom), for the boreal winter season, October – March

Temperature

When comparing the MLSO patterns (Figs. 3, 4) and the ENSO patterns (Figs. 13, 14) for temperature it is easy to see that there are large differences between their equivalent states. For example, in the strong positive state for MLSO there is mostly negative temperature anomalies over Canada but for the strong positive state for ENSO there are only positive averages (Figs. 4, 14). Then when those figures are compared to

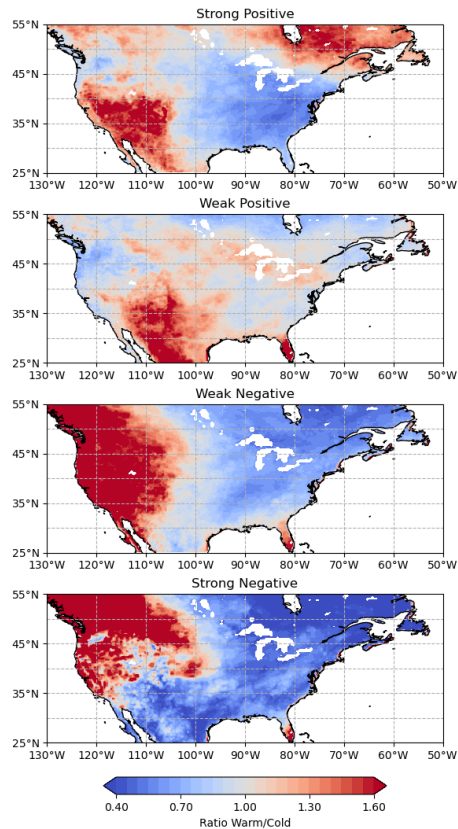


Figure 15 - The MLSO and ENSO out of phase combination, split into the bins used in figure 1, for the temperature ratios during the boreal winter, October – March

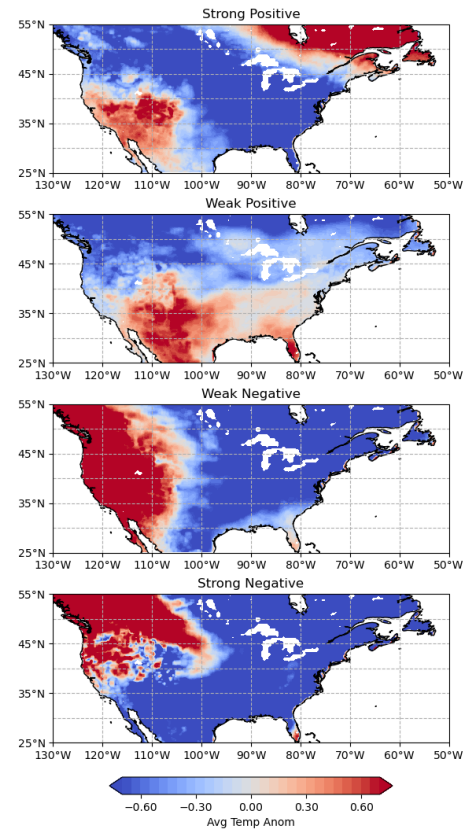


Figure 16 - The MLSO and ENSO out of phase combination, split into the bins used in figure 1, for the average temperature anomalies during the boreal winter, October – March

the combination for the out of phase boreal winter (Figs. 15, 16) more differences arise, seen in the strong positive state of the combination against the strong positive MLSO and strong negative ENSO states, the states that make up the combination. Before getting into the analysis of the combination states, the presence of temperature skewing is investigated. When comparing between the ratios and averages there are two areas of note that show a skewed temperature distribution. The first is in the strong positive

combination state in Western Canada and the second is in the weak positive bin with an area stretching from Central Canada to the area surrounding the Great Lakes. These areas of skewing show that the combination is capable of changing the “normal”, a 0° anomaly, and capable of causing more extreme temperature anomalies.

The MLSO dominates the temperature pattern in the strong positive combination state for most of the domain except over the Southwest US. ENSO dominates the temperature pattern in the Southeast US in the weak positive combination state and over the whole domain in the weak negative combination state. Also, in the weak negative combination state there is a notable amplification of the dominant ENSO pattern over western North America. Amplification also appears over the southwest US and over Mexico in the weak positive combination state, but negation also occurs in the same bin. The area of northeastern Canada, cold anomalies, shows the negation of the warm anomalies seen in both the MLSO, weak positive state, and ENSO, weak negative state, patterns. There is emergence of new patterns in the strong positive and strong negative combinations states. In the strong positive combination state (Fig. 16), MLSO – strong positive (Fig. 4) and ENSO – strong negative (Fig. 14), the area of the southwest US shows patterns of warmth that are not easily explained by either the MLSO or ENSO patterns. The same phenomenon occurs in the strong negative combination state, MLSO – strong negative and ENSO – strong positive, but occurs over western Canada, an important note for this bin is the number of days that went into this bin was 57. The rather small number of days might be helping to create a unique pattern.

What is seen in the MLSO + ENSO combination described above is seen in all the multi-oscillation analyses. The patterns of temperature for the combination states show a mixing of the patterns from the individual modes which are all unique qualitatively. An important note is that there is little to no consistency in the manner in which the MLSO interacts with the ENSO, NAO, and PNA. The locations of dominance, amplification, negation, and emergence of new patterns are different for each combination. One combination does stand out. The PNA pattern dominates the whole domain with only minor pattern shape changes when combined with the MLSO. This is probably due to the area of origin, north Pacific, for the PNA. With the MLSO only having rather minimal structure over the Pacific it is expected that the more dominant feature for the area dominates the downstream temperature patterns over North America.

Precipitation

The analysis of precipitation will focus on the MLSO + ENSO combination when the two are in phase (i.e. same sign) during boreal summer. The spatial patterns of the ratios for the MLSO (Fig. 9) and ENSO (Fig. 17) look very similar with only a few differences located over western Canada, western Mexico, and over the Atlantic. In the combination (Fig. 19) there are a few notable areas of change and dominance. When MLSO and ENSO are both in the strong positive state there is a large area of increased precipitation frequency seen over western Canada and the northwestern US indicated by the increased wet to dry ratios. There is also a large area of decreased frequency ratios over the Atlantic. For the negative combination states, weak and strong, the ENSO pattern dominates over the Atlantic, the Gulf of Mexico, and western Mexico. When the

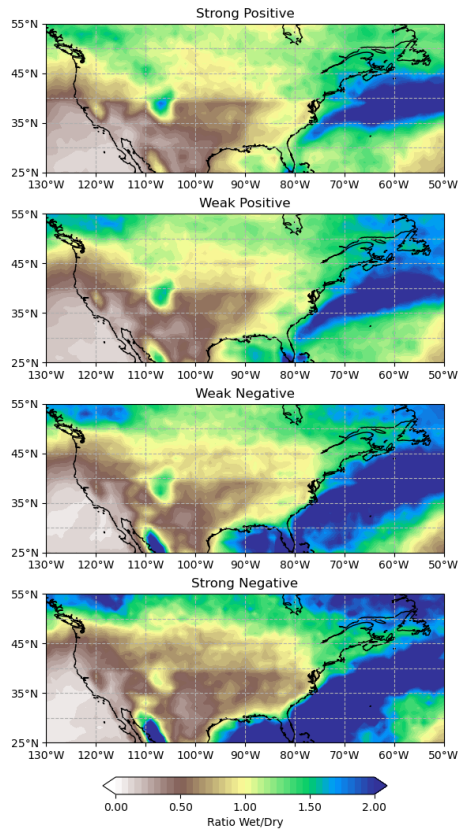


Figure 18 - The precipitation ratios for the ENSO alone, split into the index bins used in figure 1, strong positive (top) to strong negative (bottom), for the boreal summer season, April – September

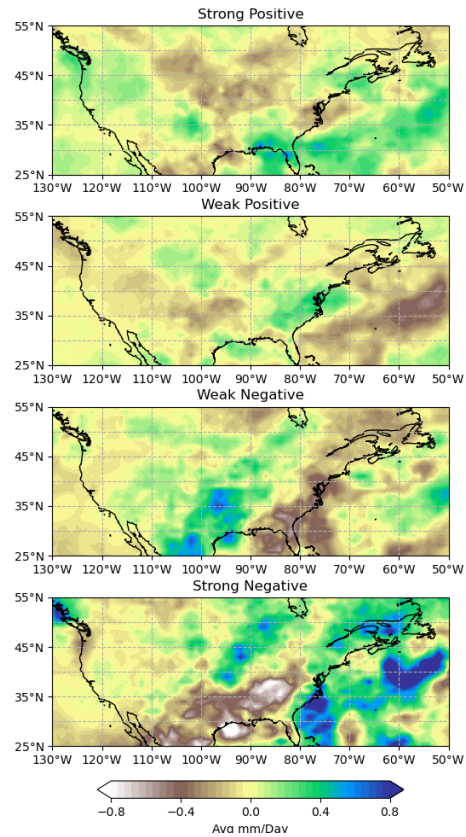


Figure 17 - The average precipitation anomalies for the ENSO alone, split into the index bins used in figure 1, strong positive (top) to strong negative (bottom), for the boreal summer season, April – September

two strong negative states are considered together, the ENSO pattern also dominates over northeastern Canada.

A much more complicated picture arises for the precipitation anomalies. The MLSO (Fig. 10) and ENSO (Fig. 18) individually have distinctly different magnitudes of the average anomalies than their combination (Fig. 20), which has larger magnitudes. The precipitation anomaly patterns for MLSO and ENSO individually are closer in magnitude

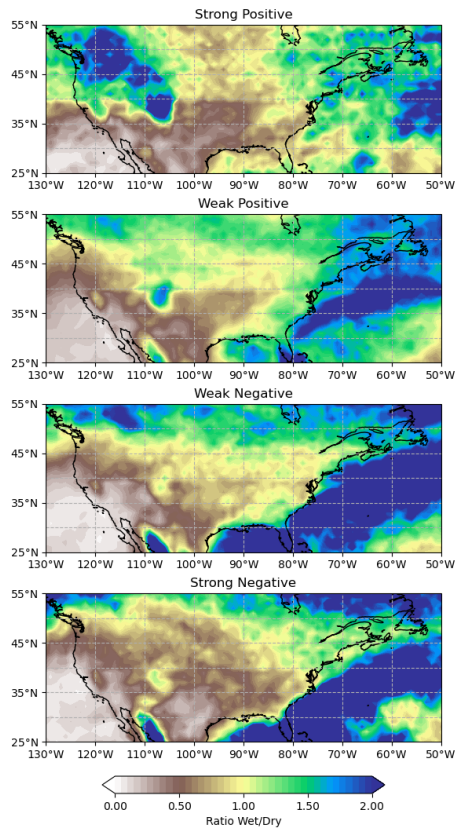


Figure 19 - The MLSO and ENSO in phase combination, split into the bins used in figure 1, for the precipitation ratios during the boreal summer, April – September

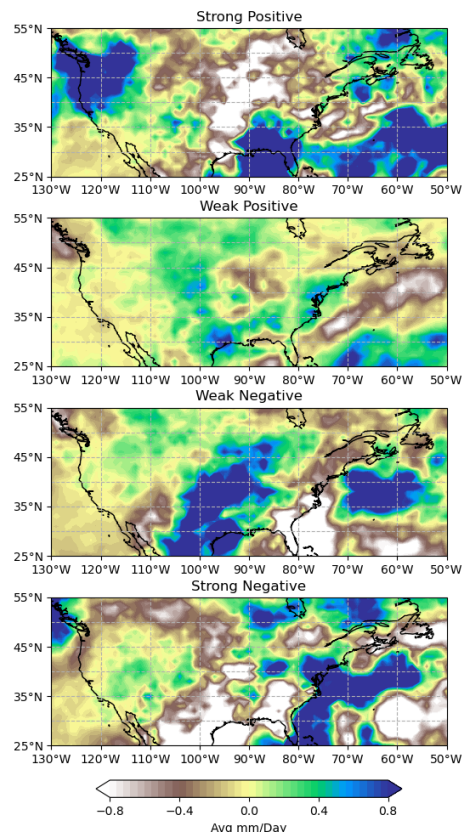


Figure 20 - The MLSO and ENSO in phase combination, split into the bins used in figure 1, for the average precipitation anomalies during the boreal summer, April – September

and spatial distribution to each other than their combination. When the MLSO and ENSO are both in their strong positive state, their combination state is very different from their individual patterns. There are areas of increased anomalies over the northwest US, southeast US, and over the Atlantic. Also, there is a large area in the central US that has decreased anomalies. When both MLSO and ENSO are in their weak negative state, the central US, Mexico, and central Atlantic have increased precipitation anomalies but the southeast US and adjacent Atlantic region have decreased anomalies. Interference occurs

when both are in their strong negative states with a decrease in anomalies over the south-central US, southeast US, and Mexico but an increase in anomalies over the Atlantic by the US east coast. In many areas of the combined MLSO and ENSO patterns manifest as an amplification of what is seen in the individual patterns. That being said, it is not a perfect aligning of patterns and there is mixing of the MLSO and ENSO patterns that creates some new patterns.

While the individual MLSO and ENSO patterns are similar for this scenario, that is not always the case. For other scenarios and combinations there can be much larger spatial variance in magnitude and pattern between the individual patterns and combination patterns. A notable combination is the MLSO + PNA combination. The dominance seen in temperature analyses of the MLSO + PNA combination during the winter also holds true for precipitation. The PNA dominance is not as strong as what is seen for the temperature analysis, as the MLSO influence on the combination states creates more deviation from the PNA patterns for precipitation. The MLSO presents itself as more of a complicating factor for precipitation. This is seen in the large number of emerging patterns that are not easily explained by either pattern for many of the MLSO and ENSO combination states and for many of the other combination states not shown. A summary of the other combinations can be found in the appendix.

CHAPTER FIVE

Discussion

The results of this study show the impact the MLSO has on the variability of temperature and precipitation over North America. The analysis of the MLSO alone revealed a strong statistical relationship between the mid-latitude oscillation and temperature over North America. For both the probability of a warm or cold day, and the magnitude of temperature anomalies, there is an MLSO pattern that comes through as significant and corroborates what was found in the research by Stan & Krishnamurthy (2019). When analyzed in combination with other sources of variability, the MLSO revealed its ability to interfere with the expected mid-latitude variability associated ENSO, NAO, and PNA. This interference is seen in the mixing of patterns of the MLSO and ENSO, NAO, or PNA that causes areas, in the combinations, to be dominated by one pattern or the other, show an amplification or negation of their patterns, and show the emergence of new patterns. The spatial patterns, of frequency ratios or anomalies, seen in this study show that for most situations the MLSO and other modes of variability could not exert dominance over the whole of North America. The exception to that is the PNA pattern during the winter which was the most dominate signal identified. MLSO interplay with the PNA during winter was only able to cause minor variations from the PNA patterns expected. Many areas show that the patterns from the MLSO and the other atmospheric modes amplified each other, seen in the MLSO + ENSO weak negative bin comparison, but there are also areas where the patterns cancel each other, as seen in the

MLSO + ENSO weak positive bin comparison. The combination of varying dominance, amplification, negation, and the emergence of new patterns clearly shows that the MLSO is an important contributor to the current state of weather over North America, both on its own and as a piece of a larger system.

A special feature that arose in this study was the areas that exhibited skewed distributions for temperature anomalies. Using the median as a proxy for the frequency ratio, it was easy to see that a separation between the median and average was common and sometimes straddled the zero mark. The skewing reveals the preference of both “normal” and extreme events in these areas. Many areas that had a warm favoring ratio and cold average, showing that the extreme cold temperatures were both larger in magnitude and more frequent as compared to extreme warm temperatures. This was most notably seen in the analysis of the MLSO winter positive bins and in the combination analysis of MLSO + ENSO in the winter out of phase positive bins.

Precipitation variability associated with the MLSO states was not statistically significant. There was little to no variability between the states for the frequency ratios, but the anomalies showed different patterns for all of the bins. While having unique precipitation anomaly patterns the only area of significance occurred over the Atlantic. The MLSO states seen in figures 9 and 10 do not show an oscillatory nature but the statistical figures, 11 and 12, do hint at a general oscillation between positive and negative states for some localized areas. When comparing patterns of precipitation associated with the combination of the MLSO and ENSO, NAO, or PNA, it is clear that the combinations can become very different from the expected individual patterns.

Analysis of the MLSO + ENSO combination (Figs. 19, 20) shows large areas where the individual patterns vary from the combination patterns for the ratios and many new patterns of anomalies with increased magnitude. The MLSO is shown to have an influence over both ratios and anomalies over North America when in combination with ENSO, NAO, or PNA and this is seen in the combinations which did not maintain the expected patterns from ENSO, NAO, and PNA. MLSO may not have a statistically significant influence over precipitation on its own but it has an ability to interfere with precipitation variability over North America.

CHAPTER SIX

Conclusion

The Mid-latitude Seasonal Oscillation is an oscillatory mode over the Northern Hemisphere that has influence over the weather. It is shown to have a statistically significant connection to temperature of North America and is a complicating factor for precipitation. The inclusion of the MLSO in forecasts and other prediction needs is a must and will help to reduce the amount of variability in weather and climate predictions that ends up being accounted for as internal variability. Knowing the MLSO has influence over North America, future research should be aimed at determining its influence over other parts of the world, especially considering the structure of the MLSO related circulation anomalies seen over Europe and Siberia. Also, the Mid-latitude Intra-Seasonal Oscillations (MLISOs) that were found by Stan & Krishnamurthy (2019), should be examined as the MLISOs may have an important role to play on a climate system as well.

APPENDIX

Appendix 1 Summary of main features for temperature anomalies for the MLSO – ENSO combination. Ratios are not discussed because of the ratio and anomaly spatial patterns are very similar

Scenario	MLSO Bin	Main Features
In Phase Summer	Strong Positive	MLSO Dominance: Eastern Canada; Emergence: Rocky Mountains and Western Canada
	Weak Positive	MLSO Dominance: Western Canada; Emergence: Eastern Canada
	Weak Negative	ENSO Dominance: Western US; Amplification: Eastern US; Negation: Eastern Canada
	Strong Negative	ENSO dominance: Mexico and Southeast US; MLSO dominance: Eastern Canada; Amplification: Western North America; Negation: Central US
Out of Phase Summer	Strong Positive	ENSO Dominance: Central & Eastern US; Negation: Western US & Eastern Canada
	Weak Positive	ENSO Dominance: Most of Domain
	Weak Negative	ENSO Dominance: North Central US
	Strong Negative	Emergence: Most of Domain
In Phase Winter	Strong Positive	ENSO Dominance: Canada & Northern US; Emergence: Southeast US & Mexico
	Weak Positive	ENSO Dominance: Most of Domain; Emergence: Central US
	Weak Negative	MLSO Dominance: Central & Western Canada & Western US; ENSO Dominance: Eastern Canada; Amplification: Most of US
	Strong Negative	MLSO Dominance: Eastern & Western Canada; Amplification: Central & Eastern US & Central Canada
Out of Phase Winter	Strong Positive	MLSO Dominance: Everywhere except Southwest US; Emergence: Southwest US
	Weak Positive	MLSO Dominance: Central & Western Canada; Amplification: South Central US; Negation: Eastern Canada
	Weak Negative	ENSO Dominance: Whole Domain; Amplification: Western North America
	Strong Negative	MLSO Dominance: Eastern Canada; ENSO Dominance: Southern US & Mexico; Negation: Great Lakes Region; Emergence: Western Canada

Appendix 2 Summary of main features for precipitation ratios and anomalies for the MLSO – ENSO combination

Scenario	MLSO Bin	Main Features
In Phase Summer	Strong Positive	Ratios: Increase – Western Canada & Northwest US; Decrease – Central Canada & Atlantic Anomalies: Increase – Northwest US, Southeast US, & Atlantic; Decrease – Central US & Central Canada
	Weak Positive	Ratios: Minimal variation Anomalies: New pattern but similar anomaly magnitude
	Weak Negative	Ratios: ENSO Dominance over Atlantic, Gulf of Mexico, & Western Mexico Anomalies: Increase – Central US, Mexico, & Central Atlantic; Decrease – Southeast US & Southern Atlantic
	Strong Negative	Ratios: ENSO Dominance over Atlantic, Gulf of Mexico, & Western Mexico Anomalies: Increase – Atlantic near US East Coast; Decrease – Central US, Southeast US, & Southeast Atlantic
Out of Phase Summer	Strong Positive	Ratios: ENSO Dominance over Atlantic, Gulf of Mexico, & Western Mexico; Decrease – Southeast US Anomalies: Increase – Canada & Atlantic; Decrease – Eastern US
	Weak Positive	Ratios: ENSO Dominance over Atlantic, Gulf of Mexico, & Western Mexico Anomalies: Increase – Central US & Central Atlantic; Decrease – Eastern US & Central to East Canada
	Weak Negative	Ratios: Minimal variation Anomalies: Increase – South of Great Lakes; Decrease – Southern US, Atlantic, & Central Canada
	Strong Negative	Ratios: Increase – Colorado & Gulf of Mexico; Decrease – Southern Atlantic & Western & Eastern Canada Anomalies: Increase – Western US, Central Canada, Most of Atlantic, Eastern Gulf of Mexico; Decrease: Central US, Eastern & Western Canada, & Atlantic off of Florida Coast
In Phase Winter	Strong Positive	Ratios: Increase – Central & Western Canada, Northern US, & Southern Atlantic; Decrease – Eastern Canada Anomalies: General ENSO Dominance; Increase – Northwestern US, Central Canada, South Central US, & Eastern Atlantic; Decrease – Strip going from the Central US to Eastern Canada
	Weak Positive	Ratios: Minimal variation Anomalies: Increase – Southeast US & adjacent Atlantic; Decrease – Western US, Central US, Northern Atlantic

	Weak Negative	Ratios: Decrease – Central Atlantic Anomalies: Increase – Great Lakes region & Southwest Atlantic; Decrease – Southeast US & Atlantic
	Strong Negative	Ratios: Minimal variation Anomalies: Increase – Northwest US
Out of Phase Winter	Strong Positive	Ratios: Minimal variation Anomalies: Increase – Atlantic; Decrease – Central US
	Weak Positive	Ratios: Minimal variation Anomalies: Increase – Central Atlantic, Northwest US, & Western Canada; Decrease – South Central to Southeast US
	Weak Negative	Ratios: Minimal variation Anomalies: Increase – Southeast US, Atlantic, & Northwest US; Decrease – Strip from Southwest US to East Canada
	Strong Negative	Ratios: Increase – Southern Atlantic; Decrease – Canada Anomalies: Increase – Southwest Coast of US; Decrease – Central US, Northwest US, & Southeast Atlantic

Appendix 3 Summary of main features for temperature anomalies for the MLSO – NAO combination. Ratios are not discussed because of the ratio and anomaly spatial patterns are very similar

Scenario	MLSO Bin	Main Features
In Phase Summer	Strong Positive	MLSO Dominance: Central & Southeast US; NAO Dominance: Western North America; Emergence: Northeast US
	Weak Positive	Many localized areas of Dominance for Both NAO and MLSO
	Weak Negative	MLSO Dominance: West Coast of US; Amplification: Eastern North America
	Strong Negative	MLSO Dominance: Central Canada & Southeast US; NAO Dominance: Western US & Eastern Canada; Emergence: Central US
Out of Phase Summer	Strong Positive	NAO Dominance: Southern US; Negation: Northeastern Canada; Emergence: Great Lakes region
	Weak Positive	MLSO Dominance: Canada; Amplification: Central US
	Weak Negative	NAO Dominance: Western Canada; Amplification: Most of North America
	Strong Negative	Very similar patterns that amplify over the whole domain
In Phase Winter	Strong Positive	MLSO Dominance: Western Half of North America; NAO Dominance: Eastern Half of North America
	Weak Positive	NAO Dominance: Central and Eastern North America

	Weak Negative	NAO Dominance: Whole of North America; Amplification: Central & Western Canada
	Strong Negative	MLSO Dominance: Eastern Canada; NAO Dominance: Eastern US; Emergence: Western North America
Out of Phase Winter	Strong Positive	Very similar patterns; Emergence: Western Canada
	Weak Positive	MLSO Dominance: Western Canada; Amplification: Eastern North America
	Weak Negative	MLSO Dominance: Western US; Amplification: Most of North America
	Strong Negative	NAO Dominance: Western US; Amplification: Most of US; Negation: Central Canada

Appendix 4 Summary of main features for precipitation ratios and anomalies for the MLSO – NAO combination

Scenario	MLSO Bin	Main Features
In Phase Summer	Strong Positive	Ratios: Increase – Eastern US & Western Mexico; Decrease – South Central US & Mexico Anomalies: Increase – Northwest US, Western Canada, Most of Eastern US; Decrease – Central US, Central to Eastern Canada, & Atlantic
	Weak Positive	Ratios: Minimal Variation Anomalies: Increase – South Central Atlantic, West Coast of Gulf of Mexico
	Weak Negative	Ratios: Minimal Variation Anomalies: Increase – Central US; Decrease – Southeast US & adjacent Atlantic
	Strong Negative	Ratios: Decrease – Southwest Atlantic Anomalies: Increase – Western US, Mexico, Eastern Canada, South East Atlantic; Decrease – Eastern US, Gulf of Mexico, & Atlantic
Out of Phase Summer	Strong Positive	Ratios: Increase – Western Canada Anomalies: Increase – Eastern Mexico, Texas & Atlantic; Decrease – Northeast US & Central Canada
	Weak Positive	Ratios: Minimal Variation Anomalies: Increase – Central US & Atlantic; Decrease – Southeast US & Eastern Canada
	Weak Negative	Ratios: Minimal Variation Anomalies: Increase – Central to Eastern US; Decrease – Atlantic
	Strong Negative	Ratios: Minimal Variation

		Anomalies: Increase – Central Canada & Gulf Stream area of the Atlantic; Decrease – Central US, Eastern & Western Canada, & Southern Atlantic
In Phase Winter	Strong Positive	Ratios: Increase – Strip from Western Gulf of Mexico to the Great Lakes Anomalies: Increase – South Central US to Eastern Canada, Southwest Coast of US, & Parts of the Atlantic; Decrease – Northwest Coast of US, Southeast US, & Gulf of Mexico to the Central Atlantic
	Weak Positive	Ratios: Increase – Gulf of Mexico Anomalies: Increase – Northwest US, South Central to Southeast US
	Weak Negative	Ratios: Minimal Variation Anomalies: Increase – Central US, Gulf of Mexico, & Atlantic; Decrease – Northwest & Eastern US
	Strong Negative	Ratios: Increase – Western & Eastern Canada & Atlantic; Decrease – Northern US Anomalies: Increase – Western US, Southeast US, Eastern Canada, & Atlantic; Decrease – Most of US & Most of Canada
Out of Phase Winter	Strong Positive	Ratios: Minimal Variation Anomalies: Decrease – Northwest US, Central US, & Northern and Southern Atlantic
	Weak Positive	Ratios: Minimal Variation Anomalies: Increase – Central to Eastern Canada; Decrease – Southeast US
	Weak Negative	Ratios: Minimal Variation Anomalies: Increase – Northwest US, Southeast US, & Southern Atlantic; Decrease – Southwest Coast of US, South Central US, & Central Atlantic
	Strong Negative	Ratios: Minimal Variation Anomalies: Increase – Central US; Decrease – Southeast US & Gulf of Mexico

Appendix 5 Summary of main features for temperature anomalies for the MLSO – PNA combination. Ratios are not discussed because of the ratio and anomaly spatial patterns are very similar.

Scenario	MLSO Bin	Main Features
In Phase Summer	Strong Positive	MLSO Dominance: Western Canada & Western Mexico; Amplification: Eastern US; Negation: Western US
	Weak Positive	MLSO Dominance: Northeastern US, Eastern Canada, & Western US; PNA Dominance: Southeast US;
	Weak Negative	Amplification: Southern US

	Strong Negative	MLSO Dominance: Southeast US; Amplification: North Central to Northeast US; Emergence: Western US
Out of Phase Summer	Strong Positive	Emergence: Most of US & Eastern Canada
	Weak Positive	PNA Dominance: Western Canada; Amplification: Southern US
	Weak Negative	MLSO Dominance: Eastern US; PNA Dominance: Most of Canada & Central US
	Strong Negative	MLSO Dominance: Eastern Canada; PNA Dominance: Most of US
In Phase Winter	Strong Positive	MLSO Dominance: Northeast Canada; PNA Dominance: Western North America
	Weak Positive	PNA Dominance: Most of North America
	Weak Negative	PNA Dominance: Western North America; Amplification: Eastern US
	Strong Negative	PNA Dominance: Most of North America
Out of Phase Winter	Strong Positive	MLSO Dominance: Northeast Canada; PNA Dominance: Central & Eastern US
	Weak Positive	MLSO Dominance: Eastern US
	Weak Negative	MLSO Dominance: Mexico & Eastern Canada; Amplification: Central US
	Strong Negative	MLSO Dominance: Northeast Canada; PNA Dominance: Most of North America

Appendix 6 Summary of main features for precipitation ratios and anomalies for the MLSO – PNA combination

Scenario	MLSO Bin	Main Features
In Phase Summer	Strong Positive	Ratios: Decrease – Atlantic Anomalies: Increase – Southeast US & Eastern & Western Canada; Decrease – Central Canada & Atlantic
	Weak Positive	Ratios: Minimal Variation Anomalies: Increase – Atlantic & Western Gulf of Mexico; Decrease – North Central US
	Weak Negative	Ratios: Minimal Variation Anomalies: Increase – North Central US; Decrease – Western Atlantic
	Strong Negative	Ratios: Minimal Variation Anomalies: Increase – Central US & Southwest Atlantic; Decrease – Eastern Canada & Gulf of Mexico

Out of Phase Summer	Strong Positive	Ratios: Increase – Colorado & Southeast US Anomalies: Increase – Central Canada & Southeast Atlantic; Decrease – Central US & Western Atlantic
	Weak Positive	Ratios: Minimal Variation Anomalies: Increase – Central US; Decrease – Eastern US & Northwestern US
	Weak Negative	Ratios: Minimal Variation Anomalies: New spatial patterns but little magnitude variation
	Strong Negative	Ratios: Minimal Variation Anomalies: Increase – Western US, Western Atlantic, & Central to Eastern Canada; Decrease – Eastern US, Mexico, Atlantic
In Phase Winter	Strong Positive	Ratios: Increase – Atlantic; Decrease – Central Canada Anomalies: PNA Dominance; Decrease – Western US
	Weak Positive	Ratios: Minimal Variation Anomalies: Increase – Gulf of Mexico; Decrease – Southern Atlantic
	Weak Negative	Ratios: Minimal Variation Anomalies: Increase – Central to Eastern North America & Northwest Coast of US
	Strong Negative	Ratios: Increase – James Bay Canada Anomalies: PNA Dominance; Increase – Southern US; Decrease – Northwest US & Eastern Canada
Out of Phase Winter	Strong Positive	Ratios: Increase – Northern US Anomalies: Increase – Western US & Eastern Canada; Decrease – Central US & Southeast US
	Weak Positive	Ratios: Minimal Variation Anomalies: Increase – Northern Atlantic; Decrease – Southeastern US
	Weak Negative	Ratios: Minimal Variation Anomalies: Increase – South Central US & Southern Atlantic; Decrease – Western Atlantic
	Strong Negative	Ratios: PNA Dominance – Northeast Pacific & Southern Atlantic Anomalies: PNA Dominance; Decrease – Eastern US & North Atlantic

REFERENCES

- Archambault, H. M., Bosart, L. F., Keyser, D., & Aiyyer, A. R. (2008). Influence of Large-Scale Flow Regimes on Cool-Season Precipitation in the Northeastern United States. *Monthly Weather Review*, 136(8), 2945–2963. <https://doi.org/10.1175/2007MWR2308.1>
- Bamston, A. G., Chelliah, M., & Goldenberg, S. B. (1997). Documentation of a highly ENSO-related sst region in the equatorial pacific: Research note. *Atmosphere-Ocean*, 35(3), 367–383. <https://doi.org/10.1080/07055900.1997.9649597>
- Bonsal, B., & Shabbar, A. (2008). Impacts of Large-Scale Circulation Variability on Low Streamflows over Canada: A Review. *Canadian Water Resources Journal*, 33(2), 137–154. <https://doi.org/10.4296/cwrj3302137>
- D’Agostino, R. B., Chase, W., & Belanger, A. (1988). The Appropriateness of Some Common Procedures for Testing the Equality of Two Independent Binomial Populations. *The American Statistician*, 42(3), 198–202. <https://doi.org/10.2307/2685002>
- Dee, D. P., Uppala, S. M., Simmons, A. J., Berrisford, P., Poli, P., Kobayashi, S., et al. (2011). The ERA-Interim reanalysis: configuration and performance of the data assimilation system. *Quarterly Journal of the Royal Meteorological Society*, 137(656), 553–597. <https://doi.org/10.1002/qj.828>
- Diaz, H. F., Hoerling, M. P., & Eischeid, J. K. (2001). ENSO variability, teleconnections and climate change. *International Journal of Climatology*, 21(15), 1845–1862. <https://doi.org/10.1002/joc.631>
- Durkee, J. D., Frye, J. D., Fuhrmann, C. M., Lacke, M. C., Jeong, H. G., & Mote, T. L. (2008). Effects of the North Atlantic Oscillation on precipitation-type frequency and distribution in the eastern United States. *Theoretical and Applied Climatology*, 94(1–2), 51–65. <https://doi.org/10.1007/s00704-007-0345-x>
- Hersbach, H., Bell, B., Berrisford, P., Hirahara, S., Horányi, A., Muñoz-Sabater, J., et al. (2020). The ERA5 global reanalysis. *Quarterly Journal of the Royal Meteorological Society*, 146(730), 1999–2049. <https://doi.org/10.1002/qj.3803>
- Huffman, G. J., Adler, R. F., Morrissey, M. M., Bolvin, D. T., Curtis, S., Joyce, R., et al. (2001). Global Precipitation at One-Degree Daily Resolution from Multisatellite Observations. *JOURNAL OF HYDROMETEOROLOGY*, 2, 15.
- Hurrell, J. W. (1995). Decadal Trends in the North Atlantic Oscillation: Regional Temperatures and Precipitation. *Science*, 269(5224), 676–679. <https://doi.org/10.1126/science.269.5224.676>
- Hurrell J.W., Dickson R.R. (2004) Climate variability over the North Atlantic. In: Stenseth N.C., Ottersen G., Hurrell J.W., Belgrano A. *Marine ecosystems and climate variation – the North Atlantic*. Oxford University Press 36: 301–326 <https://doi.org/10.1093/acprof:oso/9780198507499.001.0001>

- Kenyon, J., & Hegerl, G. C. (2008). Influence of Modes of Climate Variability on Global Temperature Extremes. *Journal of Climate*, 21(15), 3872–3889.
<https://doi.org/10.1175/2008JCLI2125.1>
- Leathers, D. J., Yarnal, B., & Palecki, M. A. (1991). The Pacific/North American Teleconnection Pattern and United States Climate. Part I: Regional Temperature and Precipitation Associations. *Journal of Climate*, 4(5), 517–528.
[https://doi.org/10.1175/1520-0442\(1991\)004<0517:TPATPA>2.0.CO;2](https://doi.org/10.1175/1520-0442(1991)004<0517:TPATPA>2.0.CO;2)
- Ning, L., & Bradley, R. S. (2014). Winter precipitation variability and corresponding teleconnections over the northeastern United States. *Journal of Geophysical Research: Atmospheres*, 119(13), 7931–7945.
<https://doi.org/10.1002/2014JD021591>
- Ning, L., Mann, M. E., Crane, R., & Wagener, T. (2012). Probabilistic Projections of Climate Change for the Mid-Atlantic Region of the United States: Validation of Precipitation Downscaling during the Historical Era*. *Journal of Climate*, 25(2), 509–526. <https://doi.org/10.1175/2011JCLI4091.1>
- Notaro, M., Wang, W.-C., & Gong, W. (2006). Model and Observational Analysis of the Northeast U.S. Regional Climate and Its Relationship to the PNA and NAO Patterns during Early Winter. *Monthly Weather Review*, 134(11), 3479–3505.
<https://doi.org/10.1175/MWR3234.1>
- Osman, M., Zaitchik, B., Badr, H., & Hameed, S. (2021). North Atlantic centers of action and seasonal to subseasonal temperature variability in Europe and eastern North America. *International Journal of Climatology*, 41(S1), E1775–E1790.
<https://doi.org/10.1002/joc.6806>
- Pegion, K., & Sardeshmukh, P. D. (2011). Prospects for Improving Subseasonal Predictions. *Monthly Weather Review*, 139(11), 3648–3666.
<https://doi.org/10.1175/MWR-D-11-00004.1>
- Stan, C., & Krishnamurthy, V. (2019). Intra-seasonal and seasonal variability of the Northern Hemisphere extra-tropics. *Climate Dynamics*, 53(7–8), 4821–4839.
<https://doi.org/10.1007/s00382-019-04827-9>
- Virtanen, P., Gommers, R., Oliphant, T. E., Haberland, M., Reddy, T., Cournapeau, D., et al. (2020). SciPy 1.0: fundamental algorithms for scientific computing in Python. *Nature Methods*, 17(3), 261–272. <https://doi.org/10.1038/s41592-019-0686-2>
- Walker, G. T. and Bliss, E. W. (1932) *World Weather*. V. *Memoirs of the Royal Meteorological Society*. 4, 53-84.
- Wallace, J. M., & Gutzler, D. S. (1981). Teleconnections in the Geopotential Height Field during the Northern Hemisphere Winter. *Monthly Weather Review*, 109(4), 784–812. [https://doi.org/10.1175/1520-0493\(1981\)109<0784:TITGHF>2.0.CO;2](https://doi.org/10.1175/1520-0493(1981)109<0784:TITGHF>2.0.CO;2)
- Wilks, D. S. (2011). *Statistical Methods in the Atmospheric Sciences*. Elsevier Science. Retrieved from <https://books.google.com/books?id=fxPiH9Ef9VoC>
- Zhang, X., Wang, J., Zwiers, F. W., & Groisman, P. Y. (2010). The Influence of Large-Scale Climate Variability on Winter Maximum Daily Precipitation over North America. *Journal of Climate*, 23(11), 2902–2915.
<https://doi.org/10.1175/2010JCLI3249.1>

BIOGRAPHY

Zachary H Manthos graduated from Annandale High School, Annandale, Virginia, in 2009. He received a Bachelor of Science from Virginia Commonwealth University in 2014 and a Bachelor of Science from George Mason University in 2017. He is a current master's student in the Climate Science program of George Mason University.